J Mol Model (2013) 19:73–82
DOI 10.1007/s00894-012-1514-0

ORIGINAL PAPER

MD simulation of self-diffusion and structure in some *n*-alkanes over a wide temperature range at high pressures

Huajie Feng · Wei Gao · Jingjing Nie · Jing Wang · Xiaojuan Chen · Liuping Chen · Xin Liu · Hans-Dietrich Lüdemann · Zhenfan Sun

Received: 10 March 2012 / Accepted: 20 June 2012 / Published online: 15 July 2012

Abstract Self-diffusion and structural properties of n-alkanes have been studied by molecular dynamics simulation in the temperature range between the melting pressure curve and 600 K at pressures up to 300 MPa. The simulated results of lower n-alkanes are in good agreement with the existing experimental data, and support the reliability of results of the simulations of self-diffusion coefficients obtained at the extreme conditions. We predict the self-diffusion coefficients for methane, ethane, propane and n-butane at the similar reduced temperatures and pressures to draw a comparison between them. Then the correlation between self-diffusion and structural properties are further investigated by calculating the coordination numbers. Moreover, we define four distances and their corresponding relative deviations to characterize the flexibility of long-chain n-alkanes. The simulated results show that the self-diffusion of n-alkane molecules is mainly affected by the close packing, and the flexibility has a strong impact on the self-diffusion of longer n-alkane molecules.

Keywords Alkane · Diffusion coefficient · Flexibility · High pressure · Molecular dynamics simulation

Introduction

Diffusion coefficients are essential to evaluate mass transfer rates, and the wide range of state and large variation of species in industrial technology development and in academic research need a great deal of diffusion data [1–4]. Generally, there are three methods to obtain diffusion coefficients: experimental determination, theoretical or empirical study and molecular dynamics simulation. It is very difficult and expensive to determine diffusion data experimentally over wide T and p ranges because of rigorous experimental condition. Also, several reliable correlation parameters needed for empirical or theoretical studies are difficult to obtain. Computer simulation which has attracted rather more attention and can be applied in much wider T and p ranges, has already become one of the most important methods for obtaining diffusion coefficients of fluids. Moreover, such simulations can render structural properties to be applied in the explanation of the transport properties [5–8].

The fluids of crude oils contain molecules with a wide range of sizes and species, and many mineral oils are mainly composed of alkanes. The composition of the oil determines its property, so it is desirable to study the diffusion and local structure of alkanes. Over the years, different methods have been employed to investigate alkanes. Harris and Trappeniers [9] reported the self-diffusion coefficients and densities for liquid methane at 110, 140 and 160 K. They found that the reduced diffusivity isotherms fell on a common curve when plotted against reduced density. Lüdemann et al. [10, 11] measured the self-diffusion coefficients for a series of alkanes between the melting pressure curve and 450 K at pressures up to 200 MPa by the application of the

Electronic supplementary material The online version of this article (doi:10.1007/s00894-012-1514-0) contains supplementary material, which is available to authorized users.

H. Feng · Z. Sun
School of Chemistry and Chemical Engineering, Hainan Normal University,
Haikou 571158, People's Republic of China

W. Gao · J. Nie · J. Wang · X. Chen · L. Chen (✉) · X. Liu
KLGHEI of Environment and Energy Chemistry, School of Chemistry and Chemical Engineering, Sun Yat-sen University,
Guangzhou 510275, People's Republic of China
e-mail: cesclp@mail.sysu.edu.cn

H.-D. Lüdemann
Institut für Biophysik und physikalische Biochemie, Universität Regensburg,
93040 Regensburg, Germany

pulsed field gradient NMR technique, and analyzed the data with the rough hard sphere and the interacting sphere model. Dymond et al. [12, 13] showed that a simultaneous fit is possible for thermal conductivity, viscosity, and self-diffusion coefficient data of *n*-alkanes up to pressure of 650 MPa, by a correlation method based on consideration of the exact hard-sphere theory of transport properties. Some molecular dynamics (MD) simulation results for the self-diffusion coefficient of *n*-butane and *n*-octane have been reported in the literature [14, 15]. Jorgensen and coworkers [16, 17] developed and tested the famous optimized potentials for liquid simulations (OPLS) potential functions for hydrocarbons through quantum chemical calculation and Monte Carlo simulations. Another common approach for *n*-alkanes is the anisotropic united atom (AUA) potential [18–20]. Krishna and van Baten used MD simulation to investigate the self-diffusivities of pure C1-C6 alkanes at 300 K for comparison with corresponding exchange coefficients in micro- and meso-porous materials [21].

Although several theoretical and experimental investigations have been devoted to pure liquid *n*-alkanes, some fascinating issues still remain. For instance, the critical temperature of methane is far lower than that of other *n*-alkanes, and the critical pressure of methane is lower than that of ethane, while the critical pressure of other *n*-alkanes decreases with increasing number of carbon. To the best of our knowledge, questions concerning the relation between the macroscopic self-diffusion and the microscopic structure of *n*-alkanes over a wide temperature and pressure range have not yet been definitively answered. For this reason, detailed knowledge of self-diffusion and structure of *n*-alkanes (In this paper, we only studied the *n*-alkanes, so the alkanes mentioned below are all *n*-alkanes.) is reported using computer simulation techniques. In this work, a set of MD simulations were performed to obtain the self-diffusion and structure for the fluid *n*-alkanes in the temperature range between the melting pressure curve and 600 K at pressures up to 300 MPa. The simulation results were compared with the known experimental data to validate our predictions, and were analyzed by the rough hard sphere (RHS) model [22]. Then, the coordination numbers were calculated to investigate the correlation between the self-diffusion and structural properties. And we define four distances and their corresponding relative deviations to study the flexibility of long-chain *n*-alkane. Finally, this work strived to clarify the correlations between molecular structure and the translational dynamics in those fluids.

Computational methods

Simulations were performed with the TINKER V4.2 molecular modeling software using the optimized potentials for liquid simulation (OPLS) force field. In order to improve the accuracy of the simulation results, there are a few differences in method details for different *n*-alkanes. We applied OPLS-AA force field for methane, and OPLS-UA force field for other *n*-alkanes. To consider whether the larger system more is in line with the measured diffusion data, in the beginning of our work, the molecule numbers of pure *n*-alkanes in the cubic simulation box were tried to be 300 and 500. Compared with observed self-diffusion coefficients, we found that the simulated diffusion data obtained from 300 molecules are close to that from 500 molecules. However, 500 molecules are time-consuming, so we only choose 500 molecules for methane, ethane and propane, while for the other *n*-alkanes, the molecule numbers in the cubic simulation box were 300. The cutoff distance of potential function was taken to be 1.0 nm. The long range electrostatic interactions were taken into account by means of the Ewald summation [23]. The Beeman algorithm for integration of the equations of motion was employed. The temperature and pressure coupling were performed with the Berendsen algorithm. The periodic boundary conditions were used for all the simulations. The time step was set to be 1 fs. Initially, runs of 2×10^6 time steps were taken to re-equilibrate the system, and then runs of 1×10^6 time steps were used to calculate the properties.

The MD simulation was performed in the *NVT* ensemble for calculating the diffusion coefficients and structural properties. The density is needed to determine the box size when performing *NVT* ensemble simulation. Correct density will help to obtain accurate self-diffusion coefficients. Therefore, it is necessary to investigate the density of *n*-alkanes. Most of the density data used in the simulation were taken from NIST Chemistry WebBook [24]. If the density data are not available in the literature, MD simulations were performed in the *NpT* ensemble for calculating the density, with runs of 8×10^6 time steps.

Results and discussion

The heat of vaporization

To confirm the parameters adopted in this work, the intermolecular potential energy was simulated and the heat of vaporization at the boiling point temperature was also calculated. Both of them are listed in Table 1, along with comparisons to the experimental values [25]. The heat of vaporizations $\Delta H_{vap} \sim -E+RT$ is calculated from the simulations, neglecting the slight change in the intramolecular energies of molecules due to gas–liquid transition [17]. Table 1 shows that the simulation results are in good agreement with experimental data.

Table 1 Average intermolecular potential energies ($kJ \cdot mol^{-1}$), heat of vaporizations ($kJ \cdot mol^{-1}$), compared with experimental heat of vaporizations at the boiling point temperature T_b

Alkanes	T_b (K)	E_{inter}	ΔH_{vap}	ΔH_{vap}(exp)
Methane	111.67	−7.09	8.02	8.19
Ethane	184.55	−13.06	14.60	14.69
Propane	231.05	−16.13	18.05	19.04
n-Butane	272.65	−19.34	21.61	22.44
n-Pentane	309.21	−22.77	25.34	25.79
n-Hexane	341.88	−26.03	28.87	28.85
n-Heptane	371.55	−29.17	32.26	31.77
n-Octane	398.82	−30.42	33.74	34.41
n-Nonane	423.97	−32.99	36.52	37.18
n-Decane	447.3	−35.41	39.13	39.58

The experimental data are taken from ref. [25]

Diffusion coefficients

The self-diffusion coefficient is calculated from the long-time limit of the mean-square displacement (MSD) by the following equation.

$$D = \lim_{t\to\infty} \frac{\left\langle [r(t) - r(0)]^2 \right\rangle}{6t}, \quad (1)$$

where $r(t)$ is the position of a molecule at time t, and the average is carried out over the time origin for autocorrelation and over all the molecules as usual.

As mentioned above, in this work, the MD simulation was performed in the *NVT* ensemble for calculating the diffusion coefficients. Additionally, we took a few tests by running in the *NVE* ensemble with the same density as *NVT* ensemble (but probably not exactly the same temperature as *NVT* ensemble). The results are listed in Supplementary materials (Supplementary Tables S-1 and S-2). It is obviously that the simulated self-diffusion coefficients in the *NVE* ensemble are about two orders of magnitude smaller than the experimental data. Because of the abnormal deviation, herein, it is inappropriate to study the *n*-alkanes in the *NVE* ensemble.

The self-diffusion coefficients of CH_4, C_2H_6, C_3H_8, *n*-C_4H_{10} obtained from MD simulation and the measured values are collected in Tables 2, 3, 4 and 5. The average relative deviations between the experimental data [10] and the simulated self-diffusion coefficients for CH_4, C_2H_6, C_3H_8, *n*-C_4H_{10} are 5.1 %, 5.4 %, 4.6 %, 5.5 % respectively. Generally, the simulation results agree well with experimental values, so we can use the simulation method to obtain the self-diffusion coefficients at very high temperatures and pressures, under which it is rather difficult to do experiment. In the present work, we predict the self-diffusion coefficients for CH_4, C_2H_6, C_3H_8, *n*-C_4H_{10} at similar reduced temperatures and pressures to make a comparison between them, under such conditions there have been no experimental data.

Additionally, we also simulated the self-diffusion coefficients for long-chain alkanes, from *n*-C_5H_{12} to *n*-$C_{10}H_{22}$, and compared the simulated data with the measured values [26] (for *n*-$C_{10}H_{22}$, compared the simulated data with the calculated data [13] simultaneously), which are listed in Tables 6, 7, 8, 9, 10 and 11. In Table 11, at low temperatures, the simulation seriously overestimates the self-diffusion coefficients, while the calculated data are in good agreement with the measured values. With increasing temperature, the relative error between the simulated data and the measured values significantly decreases, while the relative error between the calculated data and the measured values significantly increases. At high temperatures and low pressures, the calculation more overestimates the self-diffusion coefficient than the simulation does. In Tables 6, 7, 8, 9, 10 and 11, the relative deviations between the experimental data and the simulated self-diffusion coefficients for *n*-C_5H_{12} to *n*-$C_{10}H_{22}$ are all rather large, not the same as the short-chain *n*-alkanes discussed above. The relative deviation increases obviously as the carbon chain increases, or the temperature decreases, or the pressure increases. Such relative deviations are due to the flexibility of long-chain *n*-alkanes, and will be discussed later.

It is known that the critical temperature of methane (190.56 K) is much lower than that of ethane (305.33 K), propane (369.83 K) and *n*-butane (425.125 K), which is not like the series of amines being studied in the previous study

Table 2 Comparison of experimental and simulated self-diffusion coefficients *D* for methane in 10^{-9} $m^2 \cdot s^{-1}$

T (K)	11 MPa		31 MPa		107 MPa		207 MPa		300 MPa	
	Exp.	MD	Exp.	MD	Exp.	MD	Exp.	MD	Exp.	MD
295	158	165	57.4	56.2	26.1	25.7	17.7	17.2	-	13.5
364	252	267	92.3	95.1	39.2	38.5	26.2	25.0	-	19.5
403	315	328	118	118	-	45.3	-	29.4	-	23.2
454	345	416	146	153	59.3	56.2	40	36.1	-	28.1
500	-	491	-	182	-	65.5	-	41.4	-	32.9

The experimental self-diffusion coefficients are taken from ref. [10]

Table 3 Comparison of experimental and simulated self-diffusion coefficients D for ethane in 10^{-9} $m^2 \cdot s^{-1}$

T (K)	25 MPa		50 MPa		100 MPa		200 MPa		300 MPa	
	Exp.	MD	Exp.	MD	Exp.	MD	Exp.	MD	Exp.	MD
136	1.66	1.74	1.42	1.47	1.09	1.20	0.70	0.719	-	0.493
202	6.04	6.16	5.05	5.08	3.80	4.09	2.76	2.62	-	1.93
294	18.7	17.6	14.0	13.8	10.3	10.6	7.30	7.18	-	5.16
454	71.6	67.9	43.2	40.0	30.5	27.4	20.8	17.5	-	13.2
500	-	90.6	-	50.3	-	33.6	-	21.2	-	16.0

The experimental self-diffusion coefficients are taken from ref. [10]

[27]. Moreover, the critical pressure of methane (4.60 MPa) is lower than that of ethane (4.87 MPa), while the critical pressure of other *n*-alkanes decreases with increasing number of carbon. Therefore, we draw a comparison between them at the following similar reduced temperatures: 152 K (T_r=0.80) and 258 K (T_r=1.35) for methane, 243 K (T_r=0.80) and 413 K (T_r=1.35) for ethane, 294 K (T_r=0.80) and 500 K (T_r=1.35) for propane, 338 K (T_r=0.80) and 575 K (T_r=1.35) for *n*-butane. On the other hand, we choose the following similar reduced pressures: 11 MPa (p_r=2.39) and 207 MPa (p_r=45.01) for methane, 11 MPa (p_r=2.26) and 219 MPa (p_r=44.95) for ethane, 10 MPa (p_r=2.35) and 191 MPa (p_r=44.97) for propane, 9 MPa (p_r=2.37) for *n*-butane.

In Figs. 1 and 2, the influences of temperature and pressure upon the self-diffusion coefficients obtained from MD for the four *n*-alkanes at similar reduced temperatures and reduced pressures are compared. Obviously, the self-diffusion coefficients of CH_4, C_2H_6, C_3H_8, n-C_4H_{10} are approximately equal at the same reduced temperature and reduced pressure. As shown in Fig. 1, the self-diffusion coefficient decreases with increasing pressure and the trend is more pronounced at lower pressures, especially under the condition of low pressures and high temperatures. In Fig. 2, the self-diffusion coefficient increases as the temperature increases, and the trend is more pronounced at lower temperatures, especially near the critical temperature.

Description of D by the RHS model

In order to explore the nature of *n*-alkanes further, we analyzed the simulated self-diffusion coefficients for *n*-alkanes by the RHS model. The hard sphere diffusion coefficient $D_{0,HS}$ for a dilute gas composed of hard spheres is according to the theory of Chapman [28] and Enskog,

$$D_{0,\mathrm{HS}} = \frac{3}{8\rho\sigma^2}\left(\frac{k_B T}{m\pi}\right)^{1/2}, \tag{2}$$

with ρ the number density, σ the hard sphere diameter, k_B the Bolzmann's constant, T the temperature, and m the mass of the sphere. In denser fluids, correlations between the particles have to be taken into account, which is done by fitting the D_{HS} obtained from computer simulations as a function of the packing fraction $n=\rho\sigma^3$ to a polynomial [29].

$$D_{\mathrm{HS}} = D_{0,\mathrm{HS}} P(n) \tag{3}$$

$$P(n) = (1 - n/1.09)\left[1 + n^2\left(0.4 - 0.83n^2\right)\right] \tag{4}$$

In real liquids, attractive interactions as well as deviations from spherical symmetry lead via rotation-translation coupling to a retardation of translational mobility. According to Chandler [30], the experimental diffusion coefficient D_{exp} should thus correspond to the diffusion coefficient of a rough hard-sphere D_{RHS} given by

$$D_{\mathrm{exp}} \approx D_{\mathrm{RHS}} = A D_{\mathrm{HS}} \quad (A \leq 1), \tag{5}$$

where A characterizes the extent of a rotation-translation coupling. This leaves two free parameters for the description of self-diffusion data as a function of density and temperature: the diameter of the hard sphere σ and the parameter A.

Table 4 Comparison of experimental and simulated self-diffusion coefficients D for propane in 10^{-9} $m^2 \cdot s^{-1}$

T (K)	25 MPa		50 MPa		100 MPa		200 MPa		300 MPa	
	Exp.	MD	Exp.	MD	Exp.	MD	Exp.	MD	Exp.	MD
112	0.249	0.261	0.199	0.218	0.144	0.152	-	0.128	-	0.0961
203	2.79	2.94	2.37	2.47	1.821	1.80	1.186	1.35	-	1.07
294	9.095	9.08	7.036	7.45	5.65	5.68	3.832	3.94	-	3.28
453	32.9	33.5	22.8	23.1	15.97	16.0	10.63	11.8	-	9.57
500	-	45.5	-	29.3	-	19.8	-	14.2	-	11.5

The experimental self-diffusion coefficients are taken from ref. [10]

Table 5 Comparison of experimental and simulated self-diffusion coefficients D for n-butane in 10^{-9} $m^2 \cdot s^{-1}$

T (K)	5 MPa		50 MPa	
	Exp.	MD	Exp.	MD
193	1.86	2.04	1.50	1.54
251	4.75	4.66	3.56	3.45
295	7.61	7.96	5.84	5.59
332	10.8	11.5	8.08	7.55
382	20.0	18.6	12.0	10.9

The experimental self-diffusion coefficients are taken from ref. [26]

The RHS-diameter σ and rotation-translation coupling parameter A derived from the fits for n-alkanes are complied in Table 12, and they are in good agreement with published data [10, 11]. Generally, the diameter σ decreases slightly with increasing temperature, as is typical for all other substances studied [31–35], and increases with increasing number of carbon. The rotation-translation coupling parameter A includes the influence on self-diffusion coefficient of all factors ignored in the RHS model, e.g., the effect of attractive forces, deviations from spherical symmetry and anisotropic interactions. While the parameter A is smaller, there is a stronger influence of rotation-translation coupling upon the diffusion. The parameter A for n-alkanes generally increases with increasing temperature, and decreases with increasing number of carbon. It suggests that the influence of rotation-translation coupling upon the diffusion increases with decreasing temperature or increasing number of carbon.

Coordination numbers

The local structures of these fluids were further investigated in terms of coordination numbers $n(r)$ at the temperatures and pressures similar to the states of studying self-diffusion coefficients, and the $n(r)$ is calculated from the following equation.

$$n(r) = 4\pi\rho_0 \int_0^r r^2 g(r) dr, \quad (6)$$

where ρ_0 is the number density, $g(r)$ is the radial distribution functions, r represents the cut-off distance corresponding to the first minimum of the radial distribution function.

The average coordination numbers $n(r)$ of CH_4, C_2H_6, C_3H_8 and n-C_4H_{10} at the temperatures and pressures similar to the conditions of studying the self-diffusion coefficients are plotted in Figs. 3 and 4. The average coordination number of CH_4 is in good agreement with the result ($n(r)$= 12) of Habenschuss [36]. Generally, the average coordination numbers of the four alkanes are approximately equal at the same reduced temperature and reduced pressure. As shown in Fig. 3, the average coordination number increases when the pressure rises, and the trend is more pronounced at lower pressures, especially at high temperatures. In Fig. 4, the average coordination number decreases when the temperature rises, and the trend is remarkably near the critical temperature at lower pressures.

Table 6 Comparison of experimental and simulated self-diffusion coefficients D for n-pentane in 10^{-9} $m^2 \cdot s^{-1}$

T (K)	5 MPa			50 MPa		
	Exp.	MD	Dev. (%)	Exp.	MD	Dev. (%)
193	1.12	1.48	32.5	0.81	1.13	39.8
252	2.90	3.56	22.8	2.35	2.69	14.7
293	5.07	5.73	13.0	3.76	4.24	12.8
355	9.78	10.2	4.0	6.18	7.10	14.9
450	28.8	24.3	−15.5	12.2	12.9	5.8

The experimental self-diffusion coefficients are taken from ref. [26]

Table 7 Comparison of experimental and simulated self-diffusion coefficients D for n-hexane in 10^{-9} $m^2 \cdot s^{-1}$

T (K)	5 MPa			50 MPa		
	Exp.	MD	Dev. (%)	Exp.	MD	Dev. (%)
214	1.15	1.43	24.3	0.74	1.02	37.7
271	2.76	3.42	23.7	1.99	2.47	24.1
313	4.83	5.51	14.1	3.37	3.95	17.1
370	8.23	9.01	9.5	5.43	6.21	14.3
443	14.6	16.4	12.6	8.69	9.88	13.7

The experimental self-diffusion coefficients are taken from ref. [26]

Table 8 Comparison of experimental and simulated self-diffusion coefficients D for n-heptane in 10^{-9} $m^2 \cdot s^{-1}$ at saturation vapor pressure

T (K)	Exp.	MD	Dev. (%)
187	0.292	0.549	88.0
198	0.436	0.786	80.2
214	0.727	1.11	53.2
226	0.976	1.37	39.9
251	1.53	2.17	41.9
278	2.39	3.08	28.7
315	3.59	4.60	28.0
365	6.00	7.26	21.0

The experimental self-diffusion coefficients are taken from ref. [26]

Table 9 Comparison of experimental and simulated self-diffusion coefficients D for n-octane in 10^{-9} $m^2 \cdot s^{-1}$ at saturation vapor pressure

T (K)	Exp.	MD	Dev. (%)
223	0.548	0.953	73.9
251	1.06	1.59	50.4
295	2.15	3.03	40.8
354	3.93	5.45	38.7
395	6.13	7.80	27.2

The experimental self-diffusion coefficients are taken from ref. [26]

From the above analysis we find that although the critical temperature of methane is much lower than that of other alkanes, the average coordination numbers as well as the self-diffusion coefficients of the four n-alkanes are approximately equal at the same reduced temperature and reduced pressure. It shows that the distribution of molecules in the n-alkanes systems affects the self-diffusion. In other words, the p-T dependence of self-diffusion properties of such fluids originates from the evolution of their structures.

Flexibility effect

The flexibility of a chain molecule is essentially determined by the rotational behavior of the skeletal bonds and the intersegmental interactions. Free bond-rotation and weak intersegmental interactions would lead to greater flexibility. There are many angles and torsions in long-chain n-alkanes. If the angle and torsion are used to characterize the flexibility, the computational and programming costs are large. Thus, we try to find a simple way to characterize the flexibility. It is well known that the mean-square end-to-end distance is usually adopted to evaluate the flexibility of the polymer molecule. Similarly, in this work, we define four distance parameters d_{AB}, d_{AC}, d_{AM} and d_{CM} to characterize the flexibility of molecules, where A and B are the two terminal carbon atoms, C is the center of carbon chain and M is the instantaneous center of mass of carbon chain, respectively. While the number of carbon atom is odd, the center of carbon chain is just the middle carbon atom. Otherwise, the center of carbon chain is the center between the two middle carbon atoms. As described above, in this work, the temperature and pressure coupling in MD simulation were performed with the Berendsen algorithm. In order to check if the simulation results are influenced by the thermostat, a few additional calculations were performed by the Andersen algorithm and the results are listed in Supplementary materials (Supplementary Tables S-3 and S-4). Obviously, the distances which characterized the flexibility of molecules conducted by the Andersen algorithm are in good agreement with those by the Berendsen algorithm. Therefore, our results are almost not influenced by the thermostat.

The distances d_{AB}, d_{AC}, d_{AM} and d_{CM} for n-decane varied with temperature and pressure are plotted in Fig. 5. It is seen in Fig. 5a, the distances d_{AB}, d_{AC} and d_{AM} decrease with increasing temperature, while d_{CM} increases with increasing temperature. In other words, an increase in the temperature would lead to a greater transformation probability, and n-decane molecules become more curved. Thus, the flexibility of n-decane molecule increases with increasing temperature and it is similar to the trend that the flexibility of the polymer molecule increases with increasing temperature [37, 38]. In Fig. 5b, the distances d_{AB}, d_{AC} and d_{AM} increase slightly with increasing pressure, while d_{CM} decreases slightly with increasing pressure. Therefore, the flexibility increases with increasing temperature and declines with increasing pressure, and the flexibility is more affected by temperature than pressure.

Furthermore, we use the parameter r_{AB}, the relative deviations between the distances at different conditions and at corresponding initial state to study the content of variation of molecular flexibility, and r_{AB} is defined by Eq. 7.

$$r_{AB} = \frac{d_{AB}(n) - d_{AB}(i)}{d_{AB}(i)} \times 100\%, \tag{7}$$

where $d_{AB}(n)$ is the distance at different temperatures and pressures, $d_{AB}(i)$ is the distance at initial state. Of course, we can use the parameters r_{AC}, r_{AM} and r_{CM} to characterize the content of variation of molecular flexibility and carry out similar analysis.

Figure 6 shows the relative deviations r_{AB} varied with carbon number and temperature. Obviously, the deviation becomes more and more serious with increasing carbon number or increasing temperature, and it means that the n-alkane with longer chain at higher temperature has greater flexibility. From Fig. 6, we can explain why the relative deviation between the experimental data and the simulated self-diffusion coefficients for n-C_5H_{12} to n-$C_{10}H_{22}$ increases with increasing carbon number. When carbon number increases, the flexibility of carbon chain becomes larger and larger, and the carbon chain tends to become more curved. So the longer chain n-alkane is easy to exist in the

Table 10 Comparison of experimental and simulated self-diffusion coefficients D for n-nonane in 10^{-9} $m^2 \cdot s^{-1}$ at saturation vapor pressure

T (K)	Exp.	MD	Dev. (%)
226	0.379	0.704	85.6
251	0.722	1.21	68.0
278	1.18	1.88	59.3
315	2.15	2.94	36.7
365	3.92	5.10	30.1
406	5.45	7.17	31.6

The experimental self-diffusion coefficients are taken from ref. [26]

Table 11 Comparison of experimental, simulated and calculated self-diffusion coefficients D for n-decane in 10^{-9} $m^2 \cdot s^{-1}$

T (K)	5 MPa			50 MPa			100 MPa			150 MPa		
	Exp.	MD	Calc.	Exp.	MD	Calc.	Exp.	MD	Calc.	Exp.	MD	Calc.
264	0.686	1.12	0.640	-	-	-	-	-	-	-	-	-
286	1.03	1.65	1.07	0.677	1.18	0.675	-	-	-	-	-	-
314	1.60	2.34	1.79	1.13	1.71	1.17	-	-	-	-	-	-
348	2.50	3.50	2.91	1.80	2.54	1.95	1.25	1.93	1.37	-	-	-
392	3.94	5.02	4.77	2.78	3.77	3.20	2.07	2.82	2.30	1.56	2.30	1.74
448	6.24	7.87	7.86	4.20	5.50	5.08	3.14	4.24	3.70	2.46	3.36	2.86
500	-	11.0	11.7	-	7.31	7.05	-	5.46	5.10	-	-	-
600	-	22.0	23.4	-	11.8	11.1	-	8.70	7.76	-	-	-

The experimental self-diffusion coefficients are taken from ref. [26]. The calculated self-diffusion coefficients are taken from ref. [13]

coiled state, and the coiled state could slow down the self-diffusion. When this situation occurs, it is hard for the OPLS force field to describe the self-diffusion accurately, and the simulated self-diffusion coefficients overestimate the corresponding experimental data.

Figures 5 and 6 show that the flexibility increases with increasing temperature. However, the relative deviation between the experimental data and the simulated self-diffusion coefficients for n-C_5H_{12} to n-$C_{10}H_{22}$ decreases with increasing temperature. In order to explain this phenomenon, we compared the increment of self-diffusion coefficients and flexibility of n-decane with temperature and the results are shown in Fig. 7. The self-diffusion coefficients in Fig. 7a and the distances d_{CM} in Fig. 7b both increase with rising temperature. Then, we make the derivative for the self-diffusion coefficients and d_{CM}, respectively. It is seen in Fig. 7c, the derivative of self-diffusion coefficients increases with increasing temperature, while the derivative of d_{CM} decreases with increasing temperature shown in Fig. 7d. At low temperatures, while the self-diffusion is slow, although the flexibility is small, it has an important influence upon the diffusion of molecules. However, the OPLS force field parameters used in the simulation are not very exact to represent the real coiled state of molecules and their variation with temperature and pressure. Therefore, it is hard for the OPLS force field to describe the dynamics properties like the self-diffusion accurately, and the simulated self-diffusion coefficients overestimate the corresponding measured data. As the temperature rises, the flexibility increases, while the self-diffusion coefficient increases more rapidly. At high temperatures, while the self-diffusion is rather fast, although the flexibility is large comparing with that at low temperature, it only has a minor influence upon the diffusion. In other words, at high temperatures, the OPLS force field is better to describe the self-diffusion, and the simulated self-diffusion coefficients are closer to the corresponding experimental data. Moreover, the relation between the self-diffusion and flexibility varied with pressure is similar to that varied with temperature. Therefore, the flexibility leads to the

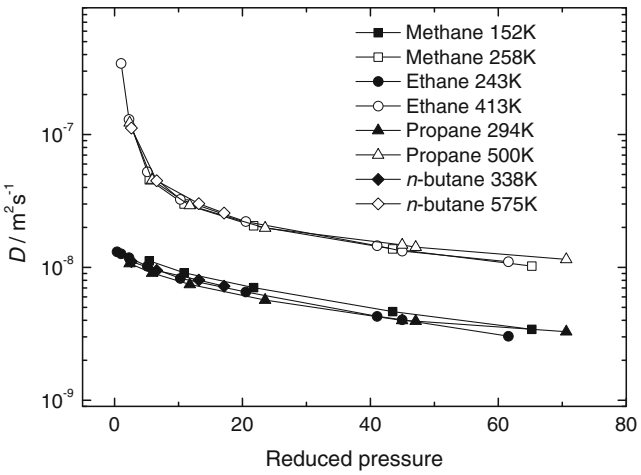

Fig. 1 Simulated self-diffusion coefficients for methane, ethane, propane and n-butane as a function of reduced pressure at two groups of similar reduced temperatures

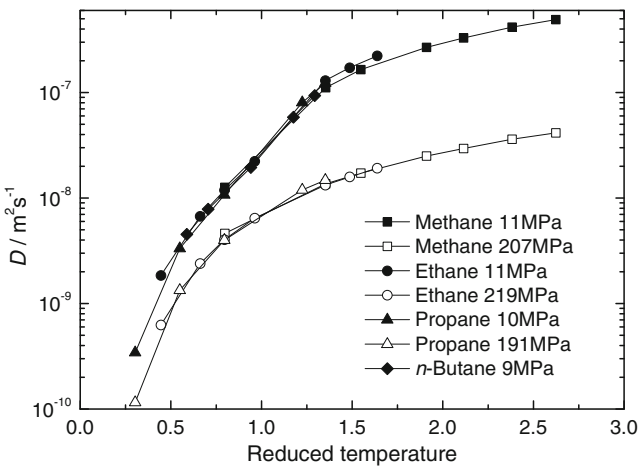

Fig. 2 Simulated self-diffusion coefficients for methane, ethane, propane and n-butane as a function of reduced temperature at two groups of similar reduced pressures

Table 12 RHS-diameter σ and parameter A derived from the fitting of D for n-alkanes

Alkanes	T (K)	A	σ (10^{-10} m)
Methane	152−500	0.95−1.06	3.59−3.41
Ethane	136−500	0.62−0.95	4.17−3.99
Propane	203−500	0.62−0.97	4.61−4.55
n-Butane	250−550	0.88−0.97	5.01−4.89
n-Pentane	250−600	0.85−0.97	5.34−5.21
n-Hexane	250−600	0.75−0.97	5.63−5.54
n-Heptane	250− 600	0.78−0.93	5.93−5.78
n-Octane	250−600	0.73−0.90	6.19−6.04
n-Nonane	250−575	0.64−0.86	6.42−6.27
n-Decane	300−600	0.69−0.83	6.62−6.49

coiled state of long-chain *n*-alkanes and has an important influence upon the self-diffusion. This analysis agrees well with the results derived in the RHS model.

Conclusions

We have carried out molecular dynamics simulations of the pure fluid *n*-alkanes in the temperature range between the melting pressure curve and 600 K at pressures up to 300 MPa. In general, the results of MD simulation for CH_4, C_2H_6, C_3H_8 and n-C_4H_{10} are in good accordance with literature self-diffusion data. It is shown that MD simulation could predict the self-diffusion coefficients of lower alkanes precisely. For the above four lower *n*-alkanes, the self-diffusion coefficients are approximately equal at the same reduced temperature and reduced pressure. Then, the simulated self-diffusion coefficients for *n*-alkanes were analyzed

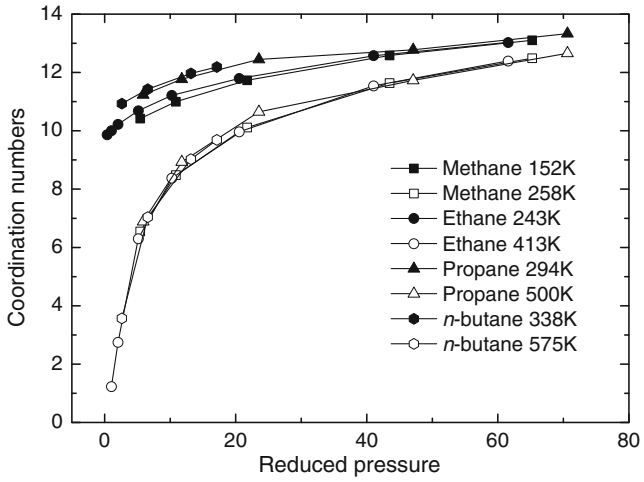

Fig. 3 The average coordination numbers n(r) of methane, ethane, propane and *n*-butane as a function of reduced pressure at two groups of similar reduced temperatures

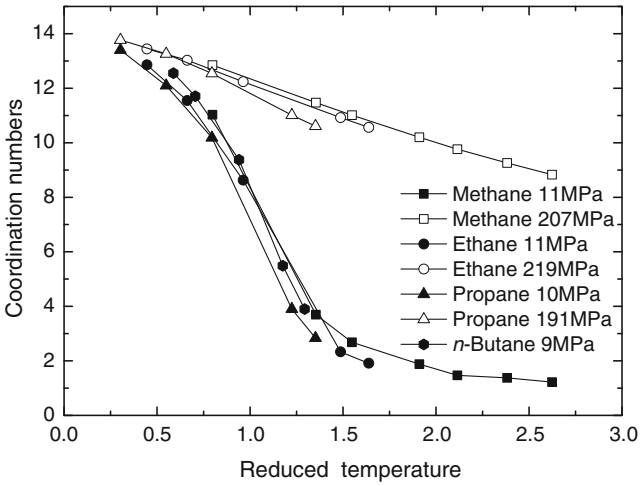

Fig. 4 The average coordination numbers n(r) of methane, ethane, propane and *n*-butane as a function of reduced temperature at two groups of similar reduced pressures

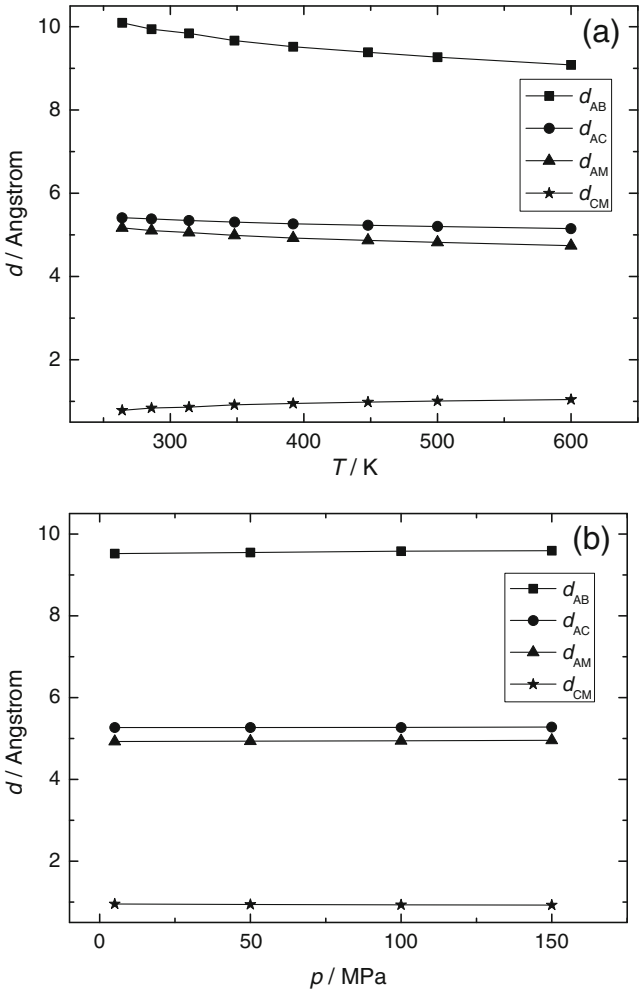

Fig. 5 The distances d_{AB}, d_{AC}, d_{AM} and d_{CM} for *n*-decane. (**a**) p= 5 MPa; (**b**) T=392 K

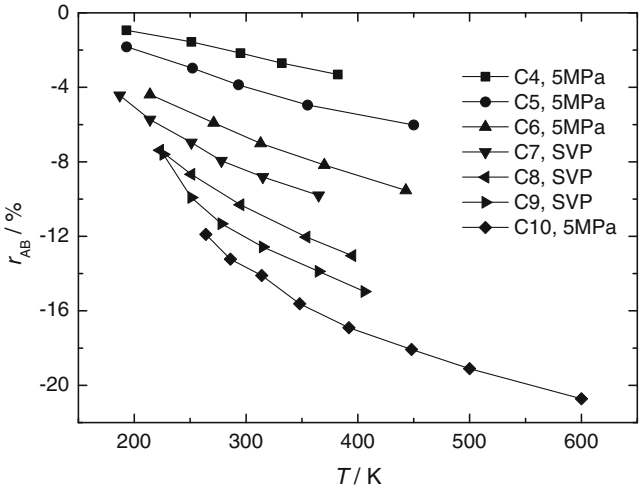

Fig. 6 The relative deviations r_{AB} for *n*-alkanes

by the rough hard sphere (RHS) model. Generally, the parameter A increases with increasing temperature, while the diameter σ decreases slightly with increasing temperature. On the other hand, the parameter A decreases with increasing number of carbon, while the diameter σ increases with increasing number of carbon.

Furthermore, the coordination numbers have been calculated to represent the internal structure of fluids. We find that the average coordination numbers of CH_4, C_2H_6, C_3H_8 and n-C_4H_{10} are approximately equal at the same reduced temperature and reduced pressure, which are consistent with the case of self-diffusion coefficients. Then the defined four distance parameters and their corresponding relative deviations can better characterize the flexibility of long-chain *n*-alkane and their variations with carbon number, temperature and pressure. At low temperatures or high pressures, the flexibility has an important influence upon the diffusion, and the simulated self-diffusion coefficients overestimate the corresponding experimental data. At high temperatures or low pressures, the flexibility has a minor influence upon the diffusion, and the simulated self-diffusion coefficients are close to the corresponding experimental data. Therefore, the p-T dependence of the self-diffusion properties of such fluids originates from the evolution of their structures, while it is mainly due to the close packing of alkane molecules, and the flexibility has a great impact on the self-diffusion of long-chain *n*-alkane molecules.

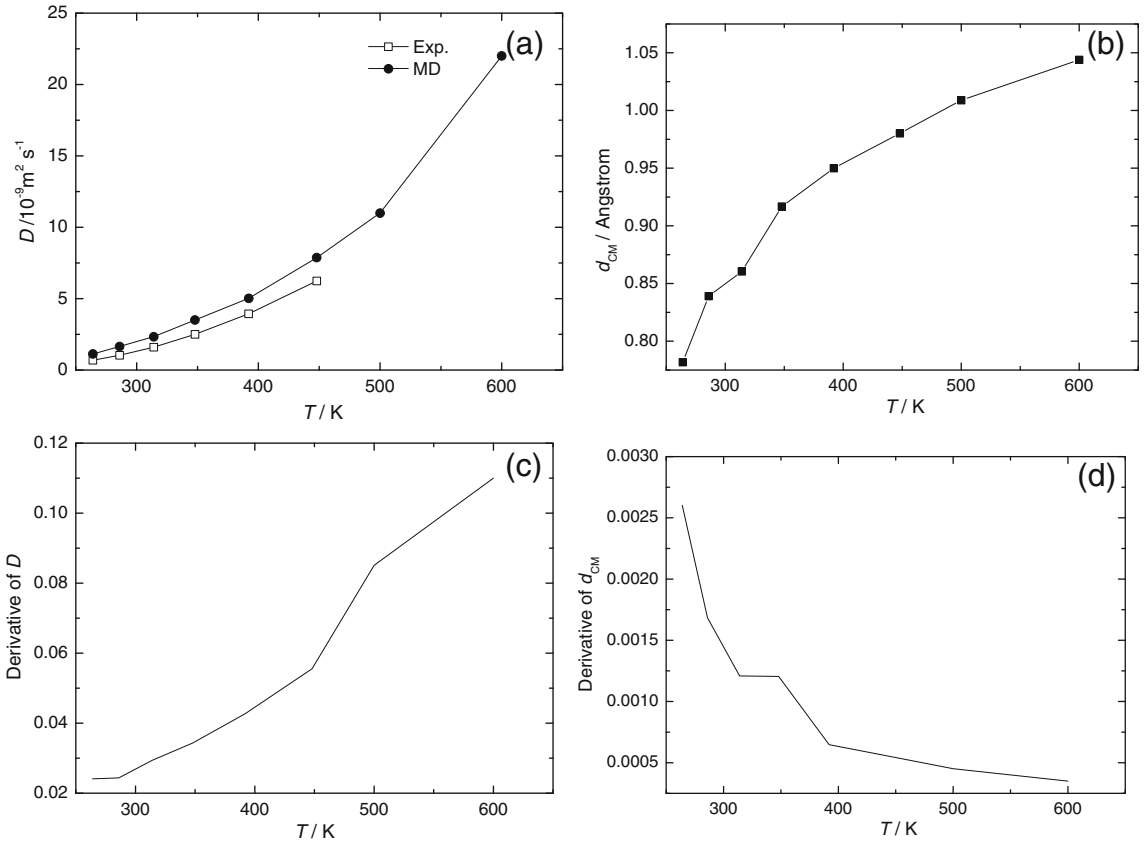

Fig. 7 Comparison between the self-diffusion coefficients and distances d_{CM} for *n*-decane. (**a**) self-diffusion coefficients D; (**b**) distances d_{CM} ; (**c**) derivative of self-diffusion coefficients; (**d**) derivative of d_{CM}

Acknowledgments The authors thank Prof. Dr. Hartmut Krienke (Universität Regensburg, Institut für Biophysik und physikalische Biochemie, D-93040 Regensburg, Germany) for the kind discussion of the paper. We also acknowledge Dr. Li Zhang working at the Zhejiang Sci-Tech University for helpful discussion about MD simulation. This work was supported by the Natural Science Foundation of Hainan Province (no. 212013, no. 212014) and the Scientific Research Foundation for Doctor and Professor of Hainan Normal University (no. 00203020218).

References

1. Zhang L, Wang Q, Liu YC et al. (2006) On the mutual diffusion properties of ethanol-water mixtures. J Chem Phys 125:104502
2. Zhao R, Macosko CW (2007) Polymer–polymer mutual diffusion via rheology of coextruded multilayers. AICHE J 53:978–985
3. Yoshida K, Matubayasi N, Nakahara M (2008) Self-diffusion coefficients for water and organic solvents at high temperatures along the coexistence curve. J Chem Phys 129:214501
4. Lin R, Tavlarides LL (2010) Diffusion coefficients of diesel fuel and surrogate compounds in supercritical carbon dioxide. J Supercrit Fluids 52:47–55
5. Fritzsche S, Gaub M, Haberlandt R et al. (1996) MD—simulation of diffusion of methane in zeolites of type LTA. J Mol Model 2:286–292
6. Zhang Y, Yang JC, Yu YX et al. (2005) Structural and hydrogen bond analysis for supercritical ethanol: a molecular simulation study. J Supercrit Fluids 36:145–153
7. Albo SE, Broadbelt LJ, Snurr RQ (2006) Multiscale modeling of transport and residence times in nanostructured membranes. AICHE J 52:3679–3687
8. Gautieri A, Mezzanzanica A, Motta A et al. (2011) Atomistic modeling of water diffusion in hydrolytic biomaterials. J Mol Model 18:1495-1502
9. Harris K, Trappeniers N (1980) The density dependence of the self-diffusion coefficient of liquid methane. Physica A 104:262–280
10. Greiner-Schmid A, Wappmann S, Has M et al. (1991) Self-diffusion in the compressed fluid lower alkanes: Methane, ethane, and propane. J Chem Phys 94:5643–5649
11. Vardag T, Bachl F, Wappmann S et al. (1990) Pressure dependence of self diffusion in some neat alkanes and binary mixtures. Ber Bunsenges Phys Chem 94:336–342
12. Dymond J, Awan M (1989) Correlation of high-pressure diffusion and viscosity coefficients for *n*-alkanes. Int J Thermophys 10:941–951
13. Assael M, Dymond J, Tselekidou V (1990) Correlation of high-pressure thermal conductivity, viscosity, and diffusion coefficients for *n*-alkanes. Int J Thermophys 11:863–873
14. Weber TA (1978) Simulation of n-butane using a skeletal alkane model. J Chem Phys 69:2347–2354
15. Weber TA (1979) Relaxation of a n-octane fluid. J Chem Phys 70:4277–4284
16. Jorgensen WL, Madura JD, Swenson CJ (1984) Optimized intermolecular potential functions for liquid hydrocarbons. J Am Chem Soc 106:6638–6646
17. Jorgensen WL, Maxwell DS, Tirado-Rives J (1996) Development and testing of the OPLS all-atom force field on conformational energetics and properties of organic liquids. J Am Chem Soc 118:11225–11236
18. Bourasseau E, Ungerer P, Boutin A et al. (2002) Monte Carlo simulation of branched alkanes and long chain *n*-alkanes with anisotropic united atoms intermolecular potential. Mol Simul 28:317–336
19. Nieto-Draghi C, Ungerer P, Rousseau B (2006) Optimization of the anisotropic united atoms intermolecular potential for *n*-alkanes: improvement of transport properties. J Chem Phys 125:044517
20. Toxvaerd S (1990) Molecular dynamics calculation of the equation of state of alkanes. J Chem Phys 93:4290–4295
21. Krishna R, Van Baten JM (2009) Unified Maxwell-Stefan description of binary mixture diffusion in micro-and meso-porous materials. Chem Eng Sci 64:3159–3178
22. Dymond J (1974) Corrected Enskog theory and the transport coefficients of liquids. J Chem Phys 60:969–973
23. Allen MP, Tildesley DJ (1987) Computer simulation of liquids. Clarendon, Oxford
24. Lemmon EW, McLinden MO, Friend DG (2009) "Thermophysical properties of fluid systems" in NIST Chemistry WebBook, NIST Standard Reference Database Number 69, Eds. National Institute of Standards and Technology, Gaithersburg MD
25. Lide DR (2010) CRC handbook of chemistry and physics, 90th ed, Internet version 2010. CRC Pr I Llc
26. Bachl F (1988) NMR-spektroskopische Untersuchungen zur Dynamik einfacher Kohlenwasserstoffe bis 600 MPa. Universität Regensburg
27. Feng H, Liu X, Gao W et al. (2010) Evolution of self-diffusion and local structure in some amines over a wide temperature range at high pressures: a molecular dynamics simulation study. Phys Chem Chem Phys 12:15007–15017
28. Chapman S, Cowling TG (1972) The mathematical theory of non-uniform gases. Cambridge University Press, Cambridge
29. Speedy R (1987) Diffusion in the hard sphere fluid. Mol Phys 62:509–515
30. Chandler D (1975) Rough hard sphere theory of the self-diffusion constant for molecular liquids. J Chem Phys 62:1358–1363
31. Ben-Amotz D, Herschbach DR (1990) Estimation of effective diameters for molecular fluids. J Phys Chem 94:1038–1047
32. Buchhauser J, Gross T, Karger N et al. (1999) Self-diffusion in CD_4 and ND_3: with notes on the dynamic isotope effect in liquids. J Chem Phys 110:3037–3042
33. Chen LP, Gross T, Lüdemann HD (1999) The density dependence of self-diffusion in some simple amines. Phys Chem Chem Phys 1:3503–3508
34. Groβ T, Buchhauser J, Price W et al. (1997) The *p*, *T*-dependence of self-diffusion in fluid ammonia. J Mol Liq 73–74:433–444
35. Karger N, Vardag T, Lüdemann HD (1990) Temperature dependence of self-diffusion in compressed monohydric alcohols. J Chem Phys 93:3437–3444
36. Habenschuss A, Johnson E, Narten AH (1981) X-ray diffraction study and models of liquid methane at 92 K. J Chem Phys 74:5234–5241
37. Guttman A, Horvath J, Cooke N (1993) Influence of temperature on the sieving effect of different polymer matrixes in capillary SDS gel electrophoresis of proteins. Anal Chem 65:199–203
38. Hou W, Yang Z (2004) Polymer physics. Chemical Industry Press, Beijing